ORGANIC LETTERS

2012
Vol. 14, No. 18
4822–4825

Core-Modified Naphthalenediimides Generate Persistent Radical Anion and Cation: New Panchromatic NIR Probes

M. R. Ajayakumar, Deepak Asthana, and Pritam Mukhopadhyay*

Supramolecular and Material Chemistry Lab, School of Physical Sciences, Jawaharlal Nehru University, New Delhi 110 067, India

**m_pritam@mail.jnu.ac.in*

Received August 1, 2012

ABSTRACT

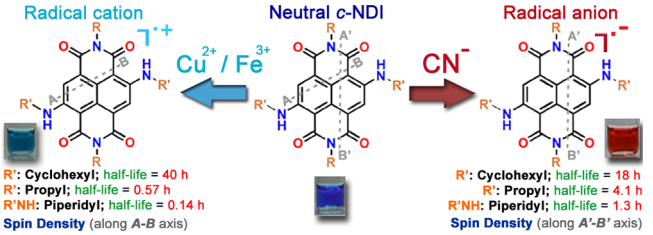

The generation of the first persistent radical cation of naphthalenediimide with Cu^{2+}/Fe^{3+} under ambient conditions is reported. An alternate anionic trigger generates a persistent radical anion within the same motif. Steric protection and H-bonding enhances the half-life of radical cation by 290-fold. The radical anion and cation have orthogonal spin density, panchromatic and NIR optical bands, which can be applied as attractive multichannel probes.

New π-extended organic radical and radical ions have attracted huge interest for their spin-based properties.[1] In contrast, their attractive low-energy optical properties in the visible (vis) and near-infrared (NIR) region due to $D_0 \rightarrow D_n$ transition have been mostly overlooked.[2] Consequently, their potential as new multichannel, wide-optical probes remains untapped, primarily because of their transient nature and complex generation processes.

Most significantly, design and synthesis of an organic π-motif that would generate a persistent radical anion as well as a cation by alternate trigger of a chemical stimulus has remained elusive. Such a molecule, by virtue of its distinct electronic levels and spin/charge distribution, would have the unique ability to harness and switch the orthogonal optical, electronic, etc. properties. This would demand (a) easily accessible HOMO and LUMO levels, (b) noninterfering functional groups for seamless gain/loss of electrons, and (c) precise structural and electronic factors to impart stability to the radical anion and cation.

Herein, we demonstrate for the first time formation of a persistent radical cation in a naphthalenediimide (NDI) moiety and simultaneous generation of radical anion by simple chemical methods, under ambient conditions. The radical cation and anion reveal orthogonal spin distribution and nonoverlapping intense absorptions in the UV, whole visible, and NIR region. Importantly, H-bonding and steric protection at the NDI-core (*c*-NDI) can enhance half-life of the radical cations by 290-fold. Furthermore, the multichannel optical properties could be applied as panchromatic, narrowband NIR probes for metal ions as well as anions having diverse charge/size.

Extensive applications of the versatile NDI moiety stem from its large π-surface and low-LUMO levels.[3,4] Our group and others have recently shown that axially

(1) (a) Torrent, M. M.; Crivillers, N.; Rovira, C.; Veciana, J. *Chem. Rev.* **2012**, *112*, 2506–2527. (b) Fukuzumi, S.; Ohkubo, K.; D'Souza, F.; Sessler, J. L. *Chem. Commun.* **2012**10.1039/C2CC32848H. (c) Miller, J. S. *Chem. Soc. Rev.* **2011**, *40*, 3266–3296. (d) Hicks, R. G. *Org. Biomol. Chem.* **2007**, *5*, 1321–1338. (e) Nishinaga, T.; Komatsu, K. *Org. Biomol. Chem.* **2005**, *3*, 561–569.

(2) Rathore, R.; Abdelwahed, S. H.; Guzei, I. A. *J. Am. Chem. Soc.* **2004**, *126*, 13582–13583.

(3) (a) Holman, G. G.; Foote, M. Z.; Smith, A. R.; Johnson, K. A.; Iverson, B. L. *Nat. Chem.* **2011**, *3*, 875–881. (b) Katz, H. E.; Lovinger, A. J.; Johnson, J.; Kloc, C.; Seigrist, T.; Li, W.; Lin, Y.-Y.; Dodabalapur, A. *Nature* **2000**, *404*, 478–481. (c) Mamada, M.; Bolvar, C. P.; Anzenbacher, P., Jr. *Org. Lett.* **2011**, *13*, 4882–4885.

(4) (a) Sakai, N.; Mareda, J.; Vauthey, E.; Matile, S. *Chem. Commun.* **2010**, *46*, 4225–4237. (b) Würthner, F.; Stolte, M. *Chem. Commun.* **2011**, *47*, 5109–5115.

10.1021/ol302140x
Published on Web 09/06/2012

modified NDI (*a*-NDI) can accept electrons from specific amines[5a] or anions[5b,c] to form persistent radical anions. However, a huge increase in NDIs gamut of applications can be anticipated if radical cation is generated within the NDI moiety. Although a wide variety of donors have been incorporated in *c*-NDI resulting in charge-separation and fascinating optical properties,[6] generation of persistent radical cation in the NDI moiety has remained elusive until now.

Toward this goal, in our design, we systematically varied the donor (D) amino units by incorporating steric, H-bonding and lipophilic groups (**1a**–**e**) (Scheme 1a). Theoretical calculations predicted a significant increase of the HOMO level to −5.5 eV (vs −7.00 eV in *a*-NDI) and an increase in the LUMO level to −3.0 eV (vs −3.8 eV in *a*-NDI).[4] **1a**–**e** were synthesized from 2,3-dibromonaphthalene-1,4,5,8-tetracarboxylic acid bisimide by reacting with the respective amines. All of the molecules were characterized in detail (Supporting Information, SI).

Scheme 1. (a) Chemical Structures (**1a**–**e**) of *c*-NDI Molecules; (b) Reaction Scheme toward Radical Anion and Radical Cation

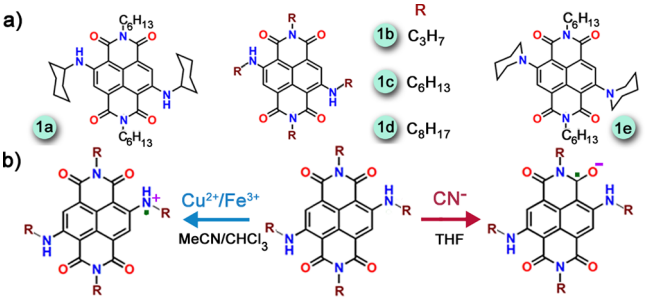

First, the ability of the *c*-NDIs to donate as well as accept electrons was verified by cyclic voltammetry (CV) and differential pulse voltammetry (DPV). Gratifyingly, **1a** show two well-separated reversible oxidation waves at +0.98 and +1.34 V and one pseudoreversible reduction wave at −0.89 V vs SCE. The experimentally determined value of HOMO and LUMO for **1a** was found to be −5.39 and −3.51 eV, respectively. Expectedly, **1b**–**e** exhibit similar redox properties, and the results are in line with similar donors (Table S1 and Figure S1, SI).[6c]

The first oxidation potential E^1_{ox} of **1a**–**e** being < 1.0 V (vs SCE), an exergonic thermal electron transfer (ET) ($\Delta G_{ET} < 0$) to Cu^{2+} to form *c*-NDI$^{\bullet+}$ can be predicted.[7]

A solvent system of MeCN/$CHCl_3$ (8:2 v/v) was required to attain uniform solubility of **1a**–**e**. The redox potential of Cu^{2+}/Cu^{+} couple was found to be +1.01 V vs SCE in this solvent system. Thus, addition of Cu^{2+} to **1a**, resulted in an instantaneous color change from deep-blue to turquoise blue. Generation of **1a**$^{\bullet+}$ was further confirmed by ESR spectroscopy with a strong signal at $g = 2.0029$ and peak-to-peak width of 10G, while with excess of Cu^{2+}, characteristic EPR signal of Cu^{2+} along with the signal of **1a**$^{\bullet+}$ was verified (Figures S2 and S3, SI).

Next, we explored the ability of **1a** to form a radical anion with reducing anions. Indeed, in the presence of cyanide anion in THF, a sharp color change from deep-blue to brown-red was observed within 10 min. The slow color transition was attributed to the endergonic ET ($\Delta G_{ET} > 0$).[7,8] **1a**$^{\bullet-}$ was confirmed by ESR with a strong resonance at $g = 2.0033$ and peak-to-peak width of 5G (Figure S2, SI). Similar results were obtained for **1b**–**e**.

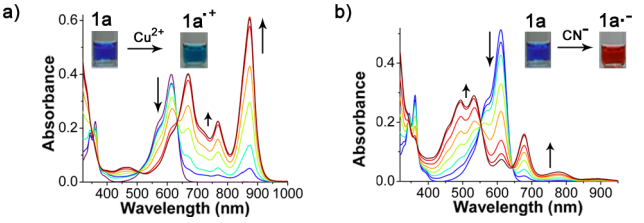

Figure 1. (a) UV–vis–NIR absorption spectra of **1a** with $Cu(ClO_4)_2$ (0–4 equiv) [**1a**; 2×10^{-4} M in MeCN/$CHCl_3$ (8:2)] and (b) **1a** with TBACN (0–4 equiv), each spectrum recorded after 30 min of equilibration [**1a**; 2×10^{-4} M in THF].

We further confirmed the formation of **1a**$^{\bullet+}$ and **1a**$^{\bullet-}$ by UV–vis–NIR absorption spectroscopy (Figure 1a,b).

Upon gradual addition of Cu^{2+} to **1a**, new bands evolved at 290, 464, 669, 768, and 874 nm with a concomitant decrease of the π–π^* 346 and 361 nm bands and the internal charge-transfer (ICT) band at 613 nm. A 1:1 stoichiometric dependence of **1a**/Cu^{2+} on the ET was confirmed (Figure S4, SI). Compounds **1b**–**d** show similar spectra upon Cu^{2+} addition, while the lowest energy band appears at 1025 nm in **1e**. The $D_0 \rightarrow D_n$ transitions qualitatively match with the calculated values (Table S2, SI).

On the other hand, with CN^- the π–π^* and ICT bands diminish with formation of new bands at 494, 533, 678, 778, and 891 nm (Figure 1b). These signature absorption bands fairly match with the theoretical results and with that of the electrochemically generated *c*-NDI$^{\bullet-}$.[9]

Importantly, the clean spectral plots and clear isosbestic points refer to uncluttered ET processes to form **1a**$^{\bullet+}$/**1a**$^{\bullet-}$. Also, significantly, the **1a**$^{\bullet+}$/**1a**$^{\bullet-}$ produce nonoverlapping

(5) (a) Ajayakumar, M. R.; Mukhopadhyay, P. *Chem. Commun.* **2009**, *25*, 3702–3704. (b) Ajayakumar, M. R.; Yadav, S.; Ghosh, S.; Mukhopadhyay, P. *Org. Lett.* **2010**, *12*, 2646–2649. (c) Guha, S.; Saha., S. *J. Am. Chem. Soc.* **2010**, *132*, 17674–17677.

(6) (a) Bhosale, S.; Sisson, A. L.; Talukdar, P.; Fürstenberg, A.; Banerji, N.; Vauthey, E.; Bollot, G.; Mareda, J.; Röger, C.; Würthner, F.; Sakai, N.; Matile, S. *Science* **2006**, *313*, 84–86. (b) Naomi, S.; Lista, M.; Kel, O.; Sakurai, S.-i; Emery, D.; Mareda, J.; Vauthey, E.; Matile, S. *J. Am. Chem. Soc.* **2011**, *133*, 15224–15227. (c) Fin, A.; Petkova, I.; Doval, D. A.; Sakai, N.; Vauthey, E.; Matile, S. *Org. Biomol. Chem.* **2011**, *9*, 8246–8252.

(7) $\Delta G_{ET} = E_{ox} - E_{red} - e^2/d\varepsilon$, in polar solvent, the Coulombic term is neglected. ΔG_{ET} (**1a**$^{\bullet+}$) = 0.98 V − 1.01 V = (−)0.03 V; E_{ox} (CN^-) = 0.87 V in THF.

(8) (a) The endergonic reaction is explained by formation of stable cyclic products from the cyanyl radical: Guo, T.; Illies, A.; Cammarata, V.; Arndt, M.; Sonzogni, W. *J. Electroanal. Chem.* **2007**, *610*, 102–105. (b) Additional stabilization is due to the well-known α-effect: Edwards, J. O.; Pearson, R. G. *J. Am. Chem. Soc.* **1962**, *84*, 16–24.

(9) Chopin, S.; Chaignon, F.; Blart, E.; Odobel, F. *J. Mater. Chem.* **2007**, *17*, 4139–4146.

intense bands in the UV−vis-NIR region. Importantly, the addition spectra of **1a**$^{\bullet+}$ and **1a**$^{\bullet-}$ cover substantial part of the solar spectra (Figure 2a). This would be highly attractive as new panchromatic,[10a] NIR dyes and for optimum solar energy utilization in solar cells.[10b]

Furthermore, **1a**$^{\bullet+}$ could regenerate **1a** upon removal of the MeCN solvent under Ar, which in turn produced the **1a**$^{\bullet-}$ upon addition of CN^- in THF (Figure 2b). The radical anion could also be switched to the radical cation upon addition of excess Cu^{2+}, making it important for applications in molecular switches, logic gates, etc.

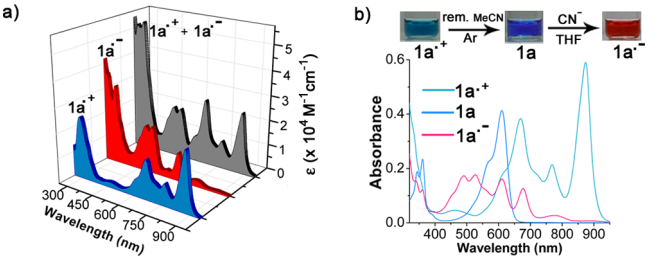

Figure 2. UV−vis−NIR absorption spectra of (a) **1a**$^{\bullet+}$, **1a**$^{\bullet-}$ and their addition spectra; (b) switching of **1a**$^{\bullet+}$ to **1a** upon removal of $MeCN/CHCl_3$ under a stream of Ar and formation of **1a**$^{\bullet-}$ with TBACN in THF.

To confirm the existence of differential spin density and charge distribution in the radical anion and cation, DFT calculations at the B3LYP/6-31+G(d,p) level of theory[11] were performed with the smallest entities of **1b**$^{\bullet+}$/**1b**$^{\bullet-}$. The spin density surface contour of **1b**$^{\bullet+}$ clearly shows that the spin is predominantly delocalized along the A-B molecular axis of **1b**$^{\bullet+}$ (Figure 3b). As expected, the two donor N atoms N21 and N22 possess the maximum spin density followed by the core-carbons C1, C5, C3, C7, C9 and C10 (Table 1). On expected lines, spin contours on the acceptor >C═O groups and the imide Ns, N13 and N18 are of negligible intensity.

In **1b**$^{\bullet-}$, the spin density is orthogonally distributed to that of **1b**$^{\bullet+}$ and is delocalized along the A′-B′ axis (Figure 3b). Core carbons C1, C4, C5, C8, and >C═O groups have major spin density.

These results are in good agreement with the resonance structures (Figure 3d,e) and support the orthogonal optical properties of *c*-NDI$^{\bullet+}$/*c*-NDI$^{\bullet-}$.The delocalized spin distribution should add to the stability of radical ions.

Next, the effect of amino substituents on the stability of radical ions was evaluated by time-dependent UV−vis-NIR analysis of the optical bands (Figure 4a). Theoretical studies along with IR, and NMR spectroscopy confirmed

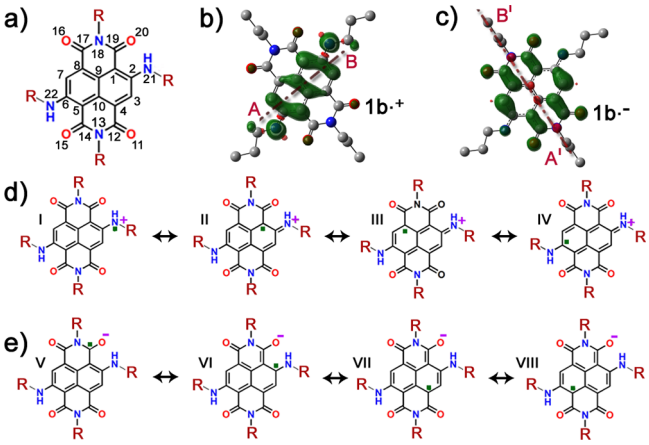

Figure 3. (a) Atom numbering scheme. Spin density of (b) **1b**$^{\bullet+}$ and (c) **1b**$^{\bullet-}$. Resonance structures of (d) *c*-NDI$^{\bullet+}$ and (e) *c*-NDI$^{\bullet-}$.

Table 1. Spin Density[a] Distributions Obtained by DFT Calculations at the B3LYP/6-31+ G (d,p) Level

	spin density			spin density	
atom	**1b**$^{\bullet+}$	**1b**$^{\bullet-}$	atom	**1b**$^{\bullet+}$	**1b**$^{\bullet-}$
C1,C5	+0.119	+0.048	C12,C17	+0.001	+0.045
C2,C6	+0.009	+0.021	N13,N18	−0.002	−0.025
C3,C7	+0.064	+0.186	C14,C19	−0.010	+0.043
C4,C8	−0.010	+0.059	O15,O20	+0.022	+0.069
C9,C10	+0.045	−0.022	N21,N22	+0.254	+0.028
O11,O16	+0.010	+0.066			

[a] Spin densities are calculated by natural population analysis. Note about the +ve/−ve signs: spin delocalization or the direct term is always positive or null, whereas the spin polarization or the indirect term is characterized by the alternation of positive or negative spin density.

intramolecular N−H---O H-bonding between the N−H and C═O groups in **1a**−**d**; e.g., the stretching frequency for the C═O group is decreased by 22 and 5 cm^{-1} in **1a** vs **1e** (SI, Figure S5). Compound **1a**$^{\bullet+}$ with bulky cyclohexyl and H-bonding donor groups was found to be the most stable and decayed slowly over a period of ten days under ambient condition. The half-life of **1a**$^{\bullet+}$ was found to be 40 h. In sharp contrast, **1b**$^{\bullet+}$−**d**$^{\bullet+}$ with considerably less bulky alkyl chains decay within 20−55 min. Compounds **1b**, **1c**, and **1d** were found to have half-lives of 0.57, 0.39, and 0.25 h, respectively. Compound **1e**$^{\bullet+}$ devoid of any H-bonding donor groups was found to be the least stable with a half-life of only 0.14 h. Therefore, steric protection[1d] of the reactive radical cation site along with H-bonding enhances the stability of **1a**$^{\bullet+}$ by 290-times in comparison to **1e**$^{\bullet+}$ (Figure 4b).

The next line of theoretical studies confirmed that intramolecular H-bonding is greatly promoted in *c*-NDI$^{\bullet+}$ with H-bond donors; e.g., the N−H, N−H---O, N---O,

(10) (a) Asthana, D.; Ajayakumar, M. R.; Pant, R. P.; Mukhopadhyay, P. *Chem. Commun.* **2012**, *48*, 6475–6477. (b) Kolemen, S.; Bozdemir, O. A.; Cakmak, Y.; Barin, G.; Ela, S. E.; Marszalek, M.; Yum, J.-H.; Zakeeruddin, S. M.; Nazeeruddin, M. K.; Grätzel, M.; Akkaya, E. U. *Chem. Sci.* **2011**, *2*, 949–954.

(11) (a) For details of DFT calculations, see the Supporting Information. (b) For Mulliken atomic charge distribution of **1a**, **1b**$^{\bullet+}$, and **1b**$^{\bullet-}$, see the Supporting Information (Table S4).

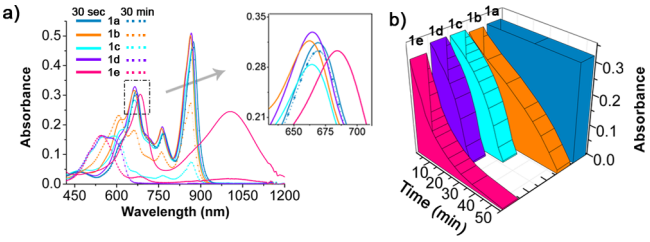

Figure 4. (a) Time-dependent UV−vis−NIR abs spectra of $\mathbf{1a}^{\bullet+}$−$\mathbf{e}^{\bullet+}$ and (b) decay profile of $\mathbf{1a}^{\bullet+}$−$\mathbf{e}^{\bullet+}$; [**1a**−**e**; 2×10^{-4} M in $MeCN/CHCl_3$ (8:2), 1 equiv of $Cu(ClO_4)$].

and C═O bond distances in $\mathbf{1b}^{\bullet+}$ were 1.027, 1.790, 2.635, and 1.236 Å, respectively, while for **1b**, the distances were 1.018, 1.845, 2.659, and 1.241 Å, respectively. In the absence of H-bonding in $\mathbf{1e}^{\bullet+}$, the N---O distance is increased to 2.870 Å and the C═O bond is shortened to 1.224 Å (Table S3, SI). In the subseries **1b**−**d**, a direct dependence of lipophilicity on the stability of $\mathbf{1b}^{\bullet+}$−$\mathbf{d}^{\bullet+}$ was observed. In going from **1b** to **d**, lipophilicity calculated from *A*log*P*[12] value increases from 3.61 to 11.79. Hence, $\mathbf{1d}^{\bullet+}$ would be more reactive compared to $\mathbf{1b}^{\bullet+}$ and $\mathbf{1c}^{\bullet+}$ driven by aggregation in this polar solvent, which explains the overall stability $\mathbf{1a}^{\bullet+} > \mathbf{1b}^{\bullet+} > \mathbf{1c}^{\bullet+} > \mathbf{1d}^{\bullet+} > \mathbf{1e}^{\bullet+}$.

Stability of the *c*-$NDI^{\bullet-}$ was also dependent on intramolecular H-bonding (Table S3, SI); e.g., the N---O distance of $\mathbf{1b}^{\bullet-}$ was 2.652 Å, significantly shortened in comparison to 2.790 Å in $\mathbf{1e}^{\bullet-}$. The effect of the N substituent and its lipophilicity on the distant imide radical anion was significantly less pronounced. Compound $\mathbf{1a}^{\bullet-}$ had a half-life of 18 h, which is 14 times greater than that of $\mathbf{1e}^{\bullet-}$ (Figure S6, SI).

Finally, we explored the panchromatic, NIR optical property of *c*-$NDI^{\bullet+}$/*c*-$NDI^{\bullet-}$ as multi-ion sensor probes (Figure 5a-d). Compound **1a** was found to be highly selective and sensitive toward Cu^{2+}/Fe^{3+}, while Na^+, K^+, Mg^{2+}, Ca^{2+}, Mn^{2+}, Co^{2+}, Ni^{2+}, Ag^+, and Pb^{2+} remained silent. Cu^{2+} was 1.5 times more selective than Fe^{3+}.[13a,b] In addition, complete fluorescence turn-off of **1a** led to detection of Cu^{2+} at 63 ppb (Figure S7, SI). Similarly, **1a** was found to be highly selective for CN^-.[13c−e] In particular, $\mathbf{1a}^{\bullet+}$ with an intense NIR band at 874 nm, ε of 30300 M^{-1} cm^{-1} and half-width ($\Delta\bar{\upsilon}_{1/2}$) of only 652 cm^{-1} (Figure S8, SI) makes it a promising probe in the NIR region.

It is to be noted that signal transduction in the NDI moiety is to a large extent dependent on the ΔG_{ET} of the

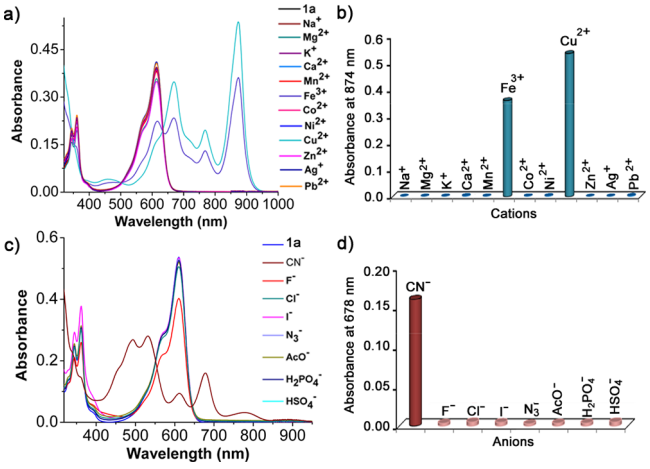

Figure 5. (a) UV−vis−NIR abs spectra and (b) selectivity profile of **1a** with different metal ions; (c) UV−vis−NIR abs spectra and (d) selectivity profile of **1a** with different anions. [**1a**; 2×10^{-4} M in $MeCN/CHCl_3$ (8:2). Metal ions: 2×10^{-4} M in $MeCN/CHCl_3$ (8:2). Anions (TBA salts): 1×10^{-3} M in THF].

redox reaction. This might limit the use of the redox probe in specific cases, e.g. in case of complete signal overlap, the identity of an oxidizing/reducing analyte has to be verified with a nonredox reference sensor.

In conclusion, the NDI moiety widely perceived as a strong π-acceptor is shown for the first time to form a persistent radical cation. With an alternate trigger the NDI moiety also forms a persistent radical anion. Incorporation of steric protection and H-bonding systematically enhances the half-life of the radical cation by 290-fold. The orthogonal spin distribution and excellent optical property of the radical ions coupled with the recent advances on *c*-NDI modification,[14] should cultivate enormous interests pervading orthogonal ET reactions, switchable organic materials and so on. We are currently working on the supramolecular aspects of these ET reactions.

Acknowledgment. We thank DBT, CSIR, DST-PURSE, and DST FIST-II for financial support, AIRF, JNU, for NMR and IR data, Mr. J. Singh, CIF, JNU, for MALDI-TOF MS, and Dr. R. P. Pant, NPL, New Delhi, for EPR. We acknowledge Dr. A. Dey, IACS, Kolkata, for his input on the theoretical calculations.

Supporting Information Available. Experimental procedures, synthesis, and various spectroscopic and theoretical data. This material is available free of charge via the Internet at http://pubs.acs.org.

(12) *A*log*P* was calculated with the software AlogPS 2.1, available from VCCLAB, http://www.vcclab.org.

(13) Cu(II) NIR probes: (a) Sanna, E.; Martínez, L.; Rotger, C.; Blasco, S.; González, J.; García-España, E.; Costa, A. *Org. Lett.* **2010**, *12*, 3840–3843. (b) Sreenath, K.; Thomas, T. G.; Gopidas, K. R. *Org. Lett.* **2011**, *13*, 1134–1137. CN^- probes: (c) Saha, S.; Ghosh, A.; Mahato, P.; Mishra, S.; Mishra, S. K.; Suresh, E.; Das, S.; Das, A. *Org. Lett.* **2010**, *12*, 3406–3409. (d) Guliyev, R.; Ozturk, S.; Sahin, E.; Akkaya, E. U. *Org. Lett.* **2012**, *14*, 1528–1531. (e) Liu, Y.; Lv, X.; Zhao, Y.; Liu, J.; Sun, Y-Q; Wang, P.; Guo, W. *J. Mater. Chem.* **2012**, *22*, 1747–1750.

(14) (a) Alvey, P. M.; Iverson, B. L. *Org. Lett.* **2012**, *14*, 2706–2709. (b) Polander, L. E.; Romanov, A. S.; Barlow, S.; Hwang, D. K.; Kippelen, B.; Timofeeva, T. V.; Marder, S. R. *Org. Lett.* **2012**, *14*, 918–921. (c) Bhosale, S. V.; Bhosale, S. V.; Bhargava, S. K. *Org. Biomol. Chem.* **2012**, *10*, 6455–6468.

The authors declare no competing financial interest.